Acta Geodyn. Geomater., Vol. 9, No. 1 (165), 71–77, 2012

THE REALIZATION OF STRONG, STRAY STATIC MAGNETIC FIELDS

Václav ŽEŽULKA* and Pavel STRAKA

Institute of Rock Structure and Mechanics, Academy of Sciences of the Czech Republic, v.v.i., V Holešovičkách 41, 182 09 Prague, Czech Republic
**Corresponding author's e-mail:* zezulka@irsm.cas.cz

(*Received* October 2011*, accepted* October 2011)

ABSTRACT
The article introduces the results achieved in the creation of feasible assemblies of NdFeB magnets assembled following an already published design of a practical arrangement of magnets derived from an ideal magnetization pattern, leading to the strongest possible stray field at a remote point. It presents a method of the implementation of these assembled sets and the relevant measured dependences of magnetic induction $B_y = f(y)$ and $B_y = f(x)$ including their comparison with already published dependences determined by a simulation. It further presents similar dependences of magnetic induction found in the case of a trial magnetic circuit with large blocks from NdFeB magnets, and these dependences are compared both with the mentioned computer-determined dependences and the dependences measured with the corresponding implemented assembly of magnets.

KEYWORDS: static magnetic fields, magnetic circuits, permanent NdFeB magnets

1. INTRODUCTION

Magnetization patterns creating a so-called one-side flux were first described by Mallinson (1973) and then further especially by Halbach (1980). A Halbach array of permanent magnets allows an increase of the magnetic field on one side of this assembly while cancelling this field on the other side. This assembly has been implemented in the magnetic systems of various devices, for instance in the case of permanent magnet brushless machines employing multipole Halbach magnetized rotors (Zhu and Howe, 2001). Arising from the Halbach cylinder, there are also publications dealing with the design and optimization of the assemblies of the permanent magnets for the generation of high magnetic fields (Bloch et al., 1998), or comparing the efficiency of various types of these assemblies for the creation of uniform fields for MRI devices (Li and Devine, 2005). Other works investigate for example the possibility of the design of the Halbach array using numerical optimization methods (Choi and Yoo, 2008) or present an algorithm for improving the difference in flux density between a high and a low magnetic-field region in an air gap in a magnetic structure and as an example applied to a two-dimensional concentric Halbach magnet design (Bjork et al., 2011).

A number of works have recently been focused on applications in NMR and MRI devices and various assemblies of permanent magnets designed. Sometimes the theoretical design with a simulation is also accompanied by a feasible prototype (Sakellariou et al., 2010), (Wang et al., 2010); other publications deal predominantly with for instance the presentation of analytical expressions for the study of magnetic fields (Ravaud and Lemarquand, 2009), properties of various magnetic configurations for an MRI magnet (Podol'skii, 1998), creation of strong, stray, static magnetic fields (Marble, 2008) or design methodology of single-side magnets (Marble, 2007). Besides the indisputable benefit of computer simulations in the design of any assembly of magnets, however, precisely knowledge and experience acquired in its practical implementation can significantly contribute to deeper knowledge and to decision-making in the further direction of development. The main reason for the implementation of a theoretically designed magnet assembly is the possibility to verify the presented parameters. Nevertheless, it is possible to present as another argument for instance also the seemingly secondary issue, which is the indispensible mastery of the great forces with which particularly NdFeB magnets of materials with high energy products and great dimensions act in the course of assembly on one another and on the surrounding ferromagnetic objects. The determination and verification of a suitable method of the assembly of such magnets is therefore a necessary condition of the implementation of designed assemblies, or circuits, already now. It is clear that with the discovery of a new generation of permanent magnets with an even substantially greater energy product as against the current NdFeB magnets the importance of the methods of their assembly increases even more significantly.

In the paper already mentioned above (Marble, 2008), Marble derives a magnetization pattern leading to the strongest possible stray field at a remote point. He presents mathematical expressions which facilitate the optimization of the dimensions of the magnet for the most efficient generation of a strong magnetic field, and further also practical magnet arrangement designs that approximate the ideal magnetization pattern. By means of computer simulations (employing Femlab 2.3 and a simulation program of 2-D final elements), the graphic dependences of flux density are further determined both in the case of the ideal magnetization pattern and the practical magnet assemblies designs mentioned. The author says in conclusion that: "By making the magnet bigger, or analogously decreasing the desired distance from the magnet to the origin, these results indicate that stray fields exceeding 1 T are possible".

2. AIM OF THE WORK

The basic aim was the implementation of the NdFeB magnet assemblies designed and discussed in the publication (Marble, 2008), the determination of the relevant dependences of magnetic induction $B_y = f(y)$ and $B_y = f(x)$ with these feasible assemblies and their comparison with the dependences determined by computer simulations, presented in the above-mentioned publication. Another objective was to determine similar magnetic-induction dependences in the case of a pilot magnetic circuit with large blocks from NdFeB magnets and compare them both with dependences from simulations and with measured dependences belonging to one of the presented magnet assemblies implemented.

3. WORK PROCEDURE

In order to generate a strong, stray magnetic field, such types of magnet assemblies were selected that can be compared with the magnet designs described by Marble (2008) in Figures 6a and 6b. For the same reason, the dimensions of these assemblies were designed so as to preserve the same proportions evident in Figure 3a (Marble, 2008). As the basis for the creation of these assemblies, NdFeB blocks from the N45 material with remanent magnetization B_r equaling 1.354 T and a maximum energy product $(BH)_{max}$ = 348 kJ/m^3 were used. The dimensions of these blocks (Ni coated) were 0.05 x 0.05 x 0.03 m, preferentially oriented in the direction of the height of 0.03 m.

The assemblies of magnets in an unmagnetized state are depicted in Figure 1 (assembly 1, corresponding to the already-mentioned design following Figure 6a) and in Figure 2 (assembly 2, corresponding to the design following Figure 6b). It is precisely assembly 2 that is a practical realization of the Halbach array with a one-side magnetic flux. The dimensional scheme of assembly 1 can be found in Figure 3a, of assembly 2 in Figure 3b. Smaller blocks

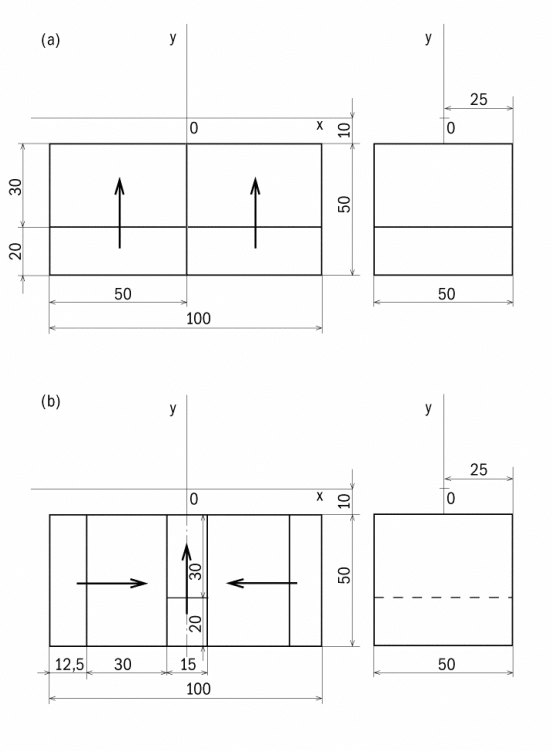

Fig. 3 Dimensional scheme of assembly 1 (a) and assembly 2 (b).

necessary for the completion of these assemblies were created by cutting from the mentioned blocks with a diamond blade under intensive cooling with water to obtain the required dimensions always in such a way as to preserve the preferential orientation for the desired block-magnetization direction.

It needs to be borne in mind that what are concerned are feasible three-dimensional assemblies, which are compared below with the designed two-dimensional designs. As however clearly arises from Figures 3a and b, the dimensions of both assemblies along axis z (not indicated in Figure 3) are 50 mm; in comparison with the dimensions along x and y, the assemblies are thus not long. As stated in (Marble, 2008), the dipole field can in such a case be reduced to two dimensions and the difference in the magnetization between the 2-D and 3-D cases is negligible. This implies that a comparison of the magnetic-induction dependences shown with the designed assemblies with those actually attained with feasible assemblies is possible in this case.

The actual magnetization was conducted along the directions indicated in Figure 3, thus in the case of the magnets of assembly 1 along axis y, with assembly 2 then magnets of the narrow central block also along axis y and the blocks on both sides along ± x.

After the individual magnets were magnetized, they were first assembled into smaller separate wholes (blocks) with the desired dimensions. In the case of

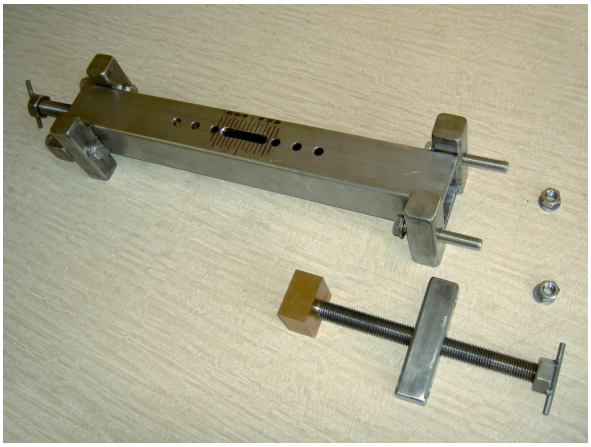

Fig. 4 The device for placing NdFeB magnets into assemblies to create a strong, stray magnetic field.

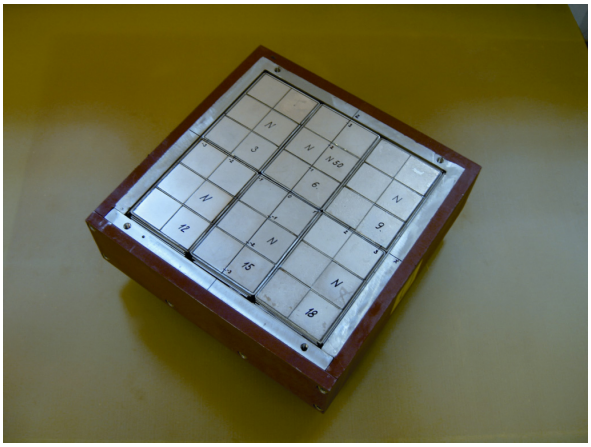

Fig. 5 Assembly 3, trial magnetic circuit.

assembly 1, two same wholes with dimensions of 50 x 50 x 50 mm were hence created, in the case of assembly 2 it was a total of three wholes, two with dimensions of 50 x 50 x 42.5 mm and one with dimensions of 50 x 15 x 50 mm. For the assembly of magnets into these wholes, a new method (Žežulka and Straka, 2007) making it possible to control the speed of the attraction of the magnets when they are approaching in the direction perpendicular to the future common contact surface was used. This method lies in the gradual insertion of the magnets into the tube of the equipment filled with a liquid (e.g. hydraulic oil), with the mutually adjacent surfaces of the magnets having the opposite polarity. The speed of attraction can then be controlled by a regulated discharge of the liquid from the space between the magnets. Since the magnets are constantly attracted to one another when they are approaching, this method also makes it possible to eliminate partial demagnetization, which can otherwise occur with another method when the magnets first repel each other when they are approaching (Žežulka and Straka, 2008).

Further completion of the mentioned smaller blocks into the respective assembly was always done in a special device, depicted in Figure 4. The device, made from stainless non-magnetics steel, makes it possible to overcome the repulsive forces, to guide the magnets when they are mutually approaching and after the assembly finishing also to measure the magnetic induction attained. In the case of assembly 1, each of the small magnetic blocks assembled is inserted from one side into the hollow steel closed square profile. The magnets were being brought closer by means of removable screws at the ends of the device which rests on the magnets across the brass supports in the shape of a block (see Fig. 4 on the right on the dismantled side of the device). In the case of assembly 2, the device is first equipped with the smallest block, which is then set in the centre of the hollow profile; subsequently, a larger block is inserted from each side. Using the screws, the center of the magnet assembly may be set precisely in the middle of the length of the square profile (point 0).

For the sake of a certain comparison with previous assemblies 1 and 2, the trial magnetic circuit shown in Figure 5 was used as assembly 3. This circuit, equipped with large blocks from NdFeB magnets originally from the N45 material, was created during previous work with the aim of achieving high values of magnetic induction in the separation zone of suspended magnetic separators as well as verifying the technology of its assembly (Žežulka, 2010). The scheme of this trial circuit including its dimensions is shown in Figure 6. Prior to the actual measurement, the circuit was in this case equipped with six large blocks from NdFeB magnets from the N50 material (B_r = 1.415 T, $(BH)_{max}$ = 384 kJ/m^3). Each block of a total weight of approximately 11 kg was assembled from three compact magnetic plates, each of which consisted of six pieces of magnets with dimensions of 50 x 50 x 30 mm. All of the magnetic plates were magnetized identically along axis y. Having been assembled, all of the blocks were of the same polarity.

It is evident that assembly 3 is a certain analog of the magnet design following Figure 6a (Marble, 2008), thus also assembly 1 in Figure 1 but with substantially greater dimensions. The free stray magnetic field here is not in the entire surroundings of the magnets, as was the case with previous assembly 1, but only in a part. As is clear from Figure 6, this trial magnetic circuit has been equipped with an iron base plate and iron side plates, whose application affects the values of the stray magnetic field in the working space above the free surface of the magnets. A certain idea of this influence is presented in (Žežulka, 2010), which in Table 2 provides the measured values and in Figure 8 the graphic dependences of magnetic induction both in the case of the circuit equipped with an iron base plate

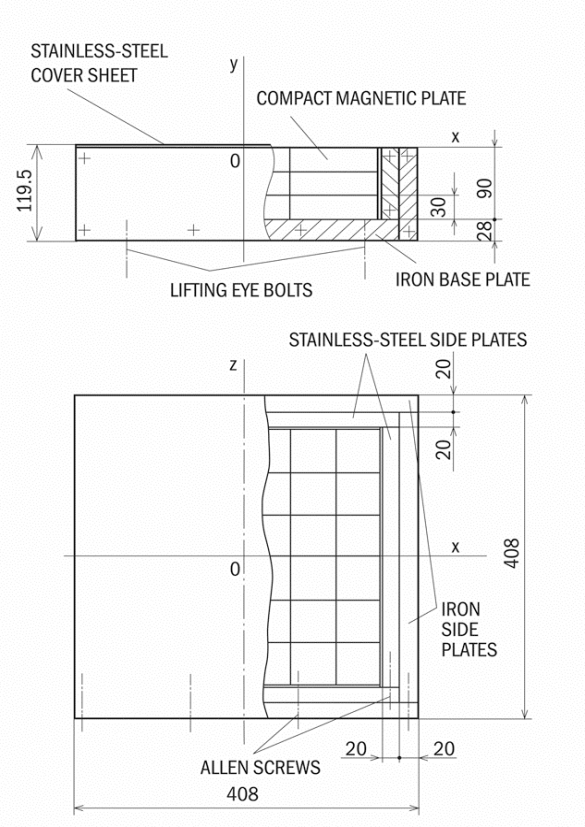

Fig. 6 Dimensional scheme of the trial magnetic circuit (Assembly 3).

and only non-magnetic stainless-steel side plates and in the case of the circuit additionally equipped with iron side plates.

4. RESULTS AND DISCUSSION

For the measurement of the magnetic-induction dependence in the case of assemblies 1 and 2, axes of the coordinates x and y were selected like in Figure 1 (Marble, 2008), just like the beginning 0 at a distance of one-tenth of the length of the magnet assembly from the surface of the magnets.

4.1. ASSEMBLIES 1 AND 2, COMPARISON OF DEPENDENCES $B_y = f(y)$

The measured dependences $B_y = f(y)$ of assemblies 1 and 2 are depicted in Figure 7. The measurement was conducted at point x = const = 0, but the maximum values at points y < 10 mm were achieved with assembly 1 at point x = const = 20 mm and with assembly 2 at point x = const = 5 mm. This phenomenon may be caused by the different magnetic properties of the magnets used, the inhomogeneity of their composition, or the Ni surface anti-corrosion protective layer.

It arises from a comparison of the values of magnetic induction B_y provided in the graph in Figure 7a in (Marble, 2008) for y in the range from -0.1 a.u. to +0.2 a.u. with the values of magnetic induction measured in the corresponding range y (from -10 mm to +20 mm) with a feasible assembly that:

Assembly 1 – In the entire range, the magnetic-induction values measured with the feasible assembly were higher than the values provided in the mentioned graph, determined by a simulation. When approaching the surface of the magnets, the difference between the value measured and the value read from the graph at the corresponding point increased. On the surface of the magnets, the maximum magnetic-induction value measured was ca 0.52 T as against the value of ca 0.25 T, read from the graph in (Marble, 2008). It is evident that with the feasible assembly the increase in magnetic induction when approaching the surface of the magnets is much more significant.

Assembly 2 – Also with the feasible assembly, the magnetic-induction values measured were higher than the values from the given graph, with their difference (determined like with assembly 1) again increasing closer to the surface of the magnets – approximately from zero at point y = 20 mm to ca 0.27 T at point -10 mm (on the surface of the magnets). The maximum actually measured magnetic induction on the surface of the magnets was ca 1.22 T, whereas the value read from the graph in (Marble, 2008) was only ca 0.95 T.

The higher magnetic-induction values measured with both assemblies are very likely to have been attained, because the magnets used had a higher remanence $B_r = 1.354$ T as against remanence $B_r = 1$ T, used in the simulation and in the creation of graphs in (Marble, 2008).

4.2. ASSEMBLIES 1 AND 2, COMPARISON OF DEPENDENCES $B_y = f(x)$ AND $|B| = f(x)$

The other dependences measured with assemblies 1 and 2 are shown in Figure 8. Unlike in the graph in Figure 7b in (Marble, 2008), showing dependence $|B| = f(x)$, however, the dependence selected for the measurement on the feasible assemblies 1 and 2 was $B_y = f(x)$, hence the dependence of only the ypsilon component of vector B on parameter x. The reason were primarily the problems with the precise measurement of the actual size B, because it was shown that a precise measurement of all three components of vector B or directly of their resultant would require an auxiliary device making it possible to set the teslameter probe precisely. Nevertheless, it arose from the measurement that in the range from -20 mm to +20 mm (corresponding to the range x from -0.2 a.u. to +0.2 a.u. in the graph in above-mentioned Figure 7b) both the values B_x and B_z are lower than B_y (e.g. $|B_x|$ with assembly 1 does not exceed ca 0.07 T), and an idea on the values of dependence $|B| = f(x)$ can thus, while bearing in mind a certain imprecision, be acquired by using dependence $B_y = f(x)$.

It arises from a comparison of magnetic induction in the graph in Figure 7b with the measured values B_y in

Figure 8 for x in ranges that mutually correspond that:

Assembly 1 – The magnetic-induction values with both dependences compared are almost constant. With the feasible assembly, the magnetic-induction values measured in the entire range were again considerably higher (approximately 0.36 T) than the values given in the graph in (Marble, 2008) (ca 0.22–0.23 T).

Assembly 2 – The induction measured at point x = 0 with the feasible assembly was slightly higher (0.56 T) than the value given in the above-mentioned graph (0.53 T). With x increasing both into positive and negative values with the feasible assembly, however, a far sharper decrease of B_y values in comparison with the values |B| given is evident. It is likely that this discrepancy is related to the increase of the B_x component, whose gradually growing values rather considerably affect the size of the resulting absolute value of magnetic induction.

4.3. ASSEMBLY 3, COMPARISON OF DEPENDENCES $B_y = f(y)$

As drawn in Figure 6, the beginning of the coordinates 0 precisely on the surface of the magnets was selected for the measurement in this case. The measured dependence $B_y = f(y)$ is shown in Figure. 9. As has been already stated above, this assembly is analogous to the assembly in Figure 6a with the respective graph in Figure 7a (squares) (Marble, 2008).

For the sake of a comparison of the measured dependence with this graph, where y is in the range from -0.1 a.u. to +0.2 a.u. (thus a total of 0.3 a.u.), the corresponding extent y and further ratios for assembly 3 were first determined. The ground-plan dimensions of the assembly of the magnets alone without the magnetic circuit were 320 x 320 mm. With the length of the assembly w = 320 mm, the corresponding range y is 0.3 x 320 = 96 mm. The maximum field can according to the legend for Fig. 3(a) (Marble, 2008) be attained with the ratio of the thickness of the magnet to its length being 0.5, which with the given length of the assembly would correspond to the height of the magnets w/2 = 160 mm. Their actual height was however only 90 mm and the corresponding ratio of the height of the magnets to their length was approximately 0.28 and as such is not optimal. Nevertheless, also with this assembly the values B_y measured in the entire range were again higher than in the graph in above-mentioned Figure 7a (squares) and also the significantly higher increase of magnetic induction when approaching the surface of the magnets, ascertained already with assembly 1, was corroborated. According to this graph, determined by simulation, the magnetic induction in the given range increases from 0.15 T only to 0.25 T on the surface of the magnets (approximate values). In the case of assembly 3 with N50 magnets with remanence B_r = 1.415 T, the magnetic induction measured in the corresponding range was from 0.25 T to almost 0.6 T on the surface of the magnets.

The influence of the extent of remanent magnetization B_r and the application of an iron magnetic circuit can be further specified with reference to the dependence in Figure 8 (Žežulka, 2010), measured on the same assembly 3 but with the N45 material of the magnets with B_r = 1.354 T, identical with the material of assemblies 1 and 2. In the same range of 96 mm, the values measured were from ca 0.19 T up to 0.585 T on the surface of the magnets, whereas when this assembly was equipped only with the iron base plate and non-magnetic side plates (i.e. without iron side plates) the values measured in the same range were from ca 0.18 T to 0.535 T.

It is obvious that the values of the magnetic induction B_y of assembly 3 mainly in the last case approximate the values $B_y = f(y)$ of assembly 1 (the values from ca 0.17 T to 0.52 T). A further correction of the magnetic induction with assembly 3 can be expected if the iron base plate is replaced with a non-magnetic plate.

4.4. ASSEMBLY 3, COMPARISON OF DEPENDENCES $B_y = f(x)$ AND $|B| = f(x)$

Like at point *B* with assemblies 1 and 2, also in this case only the values B_y were measured. The dependences $B_y = f(x)$ for various constant levels y are given in Figure 10. The range from -0.2 a.u. to +0.2 a.u. in graph 7(b) (squares) (Marble, 2008) corresponds to the range from -64 mm to +64 mm with assembly 3. At the points x = 0 and y = 30 mm (approximately corresponding to the position of the beginning 0 in Figure 3a (Marble, 2008)), the magnetic induction measured was approximately 0.36 T, at the points of ±64 mm it was ca 0.33 T – hence again higher than the corresponding data in above-mentioned graph 7(b) (squares, 0.22–0.23 T). The different shape of the curvatures of the dependences with assembly 3 as against the dependences in Figure 7b as well as in Figure 8 in the case of assembly 1 in the corresponding extent of parameter x is then very likely a result of the usage of a ferrous circuit.

5. CONCLUSIONS

The method of the realization of the designs from NdFeB magnets whose patterns were presented (including the respective magnetic-induction dependences determined by a simulation) in publication (Marble, 2008) was suggested and verified. The magnetic-induction dependences measured on feasible assemblies were compared with the dependences from this simulation. Furthermore, similar dependences were determined in the case of a trial magnetic circuit with large blocks from NdFeB magnets (assembly 3) and compared both with those calculated and the measured dependences at a feasible magnet assembly 1.

The higher measured magnetic-induction values with feasible assemblies when compared with the data

from the graphs in (Marble, 2008) may be explained by the usage of magnets with a considerably higher remanent magnetization B_r, equal to 1.354 T, or 1.415 T, than the value B_r = 1 T, used in the calculation. It can also be stated that the values of the measured magnetic-induction dependences with these feasible assemblies correspond to the dependences calculated – of course while bearing in mind the substitute $B_y = f(x)$ for $|B| = f(x)$, requiring a device for the precise measurement of the individual magnetic-induction components.

The only more significant deviation are the values of dependence $B_y = f(y)$ with both assembly 1 and assembly 3, where the increase in the measured magnetic induction is substantially greater closer to the surface of the magnets in comparison with the calculated data published.

The magnetic-induction values measured with assembly 3 corroborate the generally known fact that using a suitable type of a ferrous magnetic circuit can in a certain area further increase the magnetic induction of a stray magnetic field.

ACKNOWLEDGEMENTS

This work was supported by the Academy of Sciences of the Czech Republic as a part of the Institute Research Plan, Identification Code AVOZ30460519.

REFERENCES

Bjork, R., Bahl, C.R.H., Smith, A. and Pryds, N.: 2011, Improving magnet designs with high and low field regions. IEEE Trans. Magn., 47, no. 6, 1687–1692.

Bloch, F., Cugat, O., Meunier, G. and Toussaint, J. C.: 1998, Innovating approaches to the generation of intense magnetic fields: Design and optimization of a 4 Tesla permanent magnet. IEEE Trans. Magn., 34, no. 5, 2465–2468.

Halbach, K.: 1980, Design of permanent multipole magnets with oriented rare earth cobalt material. Nucl. Instrum. Methods, 169, issue 1, 1–10.

Choi, J. and Yoo, J.: 2008, Design of a Halbach magnet array based on optimization techniques. IEEE Trans. Magn., 44, no. 10, 2361-2366.

Li, C. and Devine, M.: 2005, Efficiency of permanent magnet assemblies for MRI devices. IEEE Trans. Magn., 41, no. 10, 3835–3837.

Mallinson, J.C.: 1973 "One-side fluxes – A magnetic curiosity?," IEEE Trans. Magn., 9, no. 4, 678–682.

Marble, A. E., Mastikhin, I. V., Colpitts B. G. and Balcom, B. J.: 2007, Designing static fields for unilateral magnetic resonance by a scalar potential approach. IEEE Trans. Magn., 43, no. 5, 1903–1911.

Marble, A. E.: 2008, Strong, stray static magnetic fields. IEEE Trans. Magn., 44, no. 5, 576-580.

Podol'skii, A.: 1998, Development of permanent magnet assembly for MRI devices., IEEE Trans. Magn., 34, no. 1, 248–252.

Ravaud, R. and Lemarquand, G.: 2009, Magnetic field in MRI yokeless devices: analytical approach. Progress in Electromagnetic Research, PIER 94, 327–341.

Sakellariou, D., Hugon, C., Guiga, A., Aubert, G., Cazaux, S. and Hardy, P.: 2010, Permanent magnet assembly producing a strong tilted homogeneous magnetic field: towards magic angle field spinning NMR and MRI. Magnetic Resonance in Chemistry, 48, no. 12, 903–908.

Wang, Z., Yang, W. H., Zhang, X. B., Hu, L. L. and Wang, H. X.: 2010, A design of 1.5 T permanent magnet for MR molecular imaging. IEEE Trans. Appl. Supercond., 20, no. 3, 777–780.

Zhu, Z.Q. and Howe, D.: 2001, Halbach permanent magnet machines and applications: A review. IEE Proc. – Electr. Power Appl., 148, no. 4, 299–308.

Žežulka, V. and Straka, P.: 2007, A new method of assembling large magnetic blocks from permanent NdFeB magnets. Acta Geodyn. Geomater., 4, no. 3 (147), 75–83.

Žežulka, V. and Straka, P.: 2008, Methods of assembling large magnetic blocks from NdFeB magnets with a high value of $(BH)_{max}$ and their influence on the magnetic induction reached in an air gap of a magnetic circuit. IEEE Trans. Magn., 44, no. 4, 485–491.

Žežulka, V.: 2010, Magnetic circuit with large blocks from NdFeB magnets for suspended magnetic separators. Acta Geodyn. Geomater., 7, no. 2 (158), 227–235.

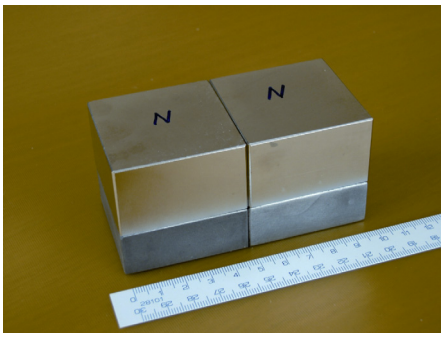

Fig. 1 Assembly 1.

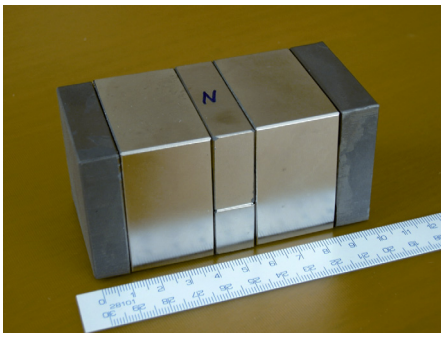

Fig. 2 Assembly 2.

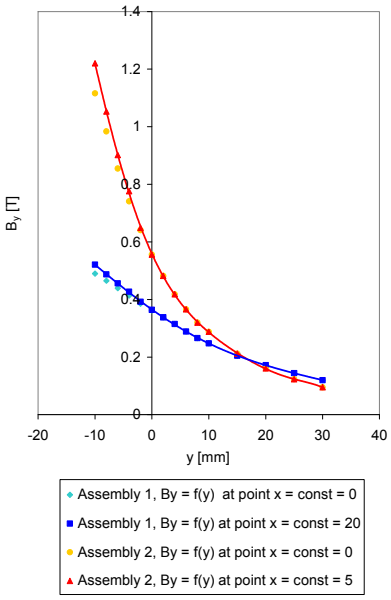

Fig. 7 Dependence $B_y = f(y)$ for assemblies 1 and 2.

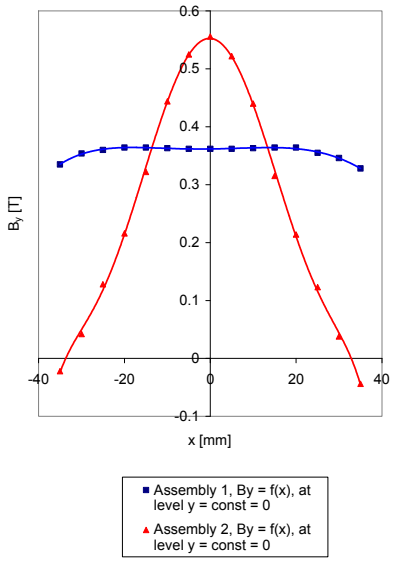

Fig. 8 Dependence $B_y = f(x)$ for assemblies 1 and 2.

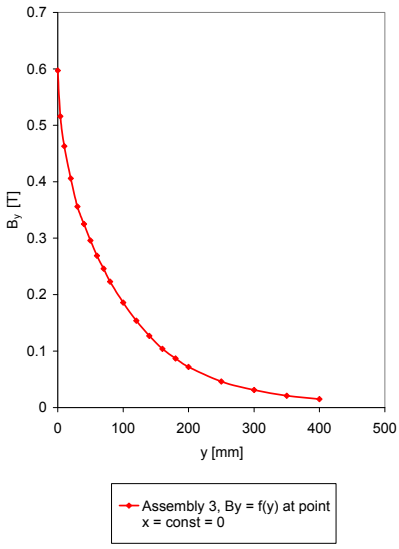

Fig. 9 Dependence $B_y = f(y)$ for assembly 3.

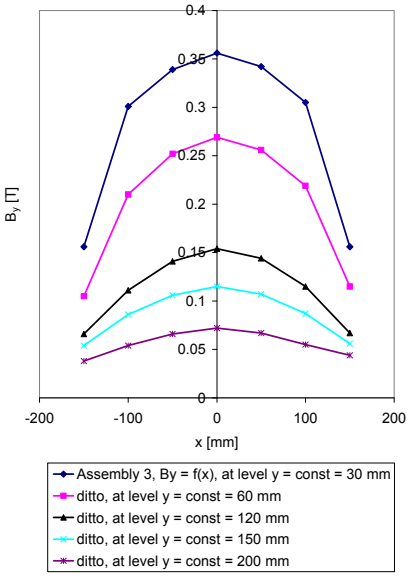

Fig. 10 Dependence $B_y = f(x)$ for assembly 3.